EVALUATING IMATINIB'S AFFINITY AND SPECIFICITY FOR MULTIPLE KINASES FROM THE BOUND-STATE USING MOLECULAR DYNAMICS SIMULATIONS

By

William Satoh Troxel

A capstone project submitted for Graduation with University Honors

May 12, 2023

University Honors

University of California, Riverside

APPROVED

Dr. Chia-en Chang

Department of Chemistry

Dr. Richard Cardullo, Howard H Hays Jr. Chair

University Honors

ABSTRACT

Computational proteomics lets us model drug-protein interactions in ways conventional assays cannot. Most drugs are specific for one protein, but some interact with multiple. One example is imatinib, which inhibits ABL to treat chronic myeloid leukemia. It binds to other kinases to treat other malignancies, but its atomistic mechanisms are poorly understood. Although complex structures are available in the Protein Data Bank, they do not show binding dynamics and protein functions. Imatinib has differential kinase affinities compared to structural similarity, ABL and SRC share 50% similarity, but a 3000x affinity difference. In contrast, ABL and KIT share 30% similarity and have strong imatinib affinities. My goals are to model free protein and imatinib-bound states for ABL, KIT, LCK, p38α, and SRC kinases using 500 ns Molecular Dynamics (MD) simulations to survey the complex interactions and conformational changes over time. The results generally agree with previous results, showing that molecular simulations are a useful method to identify the non-covalent interactions between imatinib and kinases. These simulations may serve as a useful predictor of drug affinity, as the longevity of the non-covalent interactions correspond with how well the drug sticks in the binding pocket.

ACKNOWLEDGEMENTS

I would like to thank Dr. Chia-en Chang for her generous help and support providing an opportunity to conduct undergraduate research. I would like to thank current and former members of the Chang Lab (Jianan Sun, Emily Vig, and Talant Ruzmetov) for their guidance, feedback, and assistance as I refined my research techniques, experimental design, and analysis. I would like to thank my family and friends for their continued support as I progressed through the Capstone.

I would like to thank the Research in Science and Engineering (RISE) research program, the MARC U STAR research program, and University Honors for providing additional financial support as I progress through undergraduate research.

This project was supported by Award Number T34GM062756 from the National Institutes of Health.

TABLE OF CONTENTS

INTRODUCTION

The Importance of Computational Chemistry

Computational chemistry is important because it lets researchers visualize and quantify molecular motions, interactions, and kinetics in ways that conventional bench chemistry techniques cannot show. According to the United States Food and Drug Administration (FDA), drug discovery productivity has declined since the 2000s (Paul et al., 2010). Fewer viable compounds are being discovered despite greater expenditures from government agencies, pharmaceutical companies, and biotechnology firms for their search. Conventional techniques to search for viable small compounds include high-throughput screening. High-throughput screening tests many small compounds on large cell assays to isolate compounds with observed significant effects on a biological target, making them costly and time-consuming. They usually do not have a targeted approach and produce many false positives, signifying a high failure rate (Rahman, 2015). After this, the drug candidate must go through years of expensive testing on animals and humans before it may be considered for FDA approval. Clinical testing costs over 60% of the overall cost of drug development as of 2006 (Lawrence, 2007). Therefore, a better approach is necessary for drug design. Computers may mitigate costs by using molecular models to study how existing drugs affect off-target proteins with similar binding sites and predict their binding / unbinding affinities using molecular simulations (Druker, 2004) (Ashburn & Thor, 2004) (Kinnings et al., 2009) (Jorgensen, 2004). Therefore, using computational chemistry to study how existing drugs would interact with other protein targets is a more efficient method to expand their applications since those drugs have known toxicology and history.

Chronic Myeloid Leukemia's Impact on Populations

Chronic Myeloid Leukemia (CML) accounts for about 15% of all diagnosed adult leukemia cases (Granatowicz et al., 2015) (Jabbour and Kantarijan, 2020). It is defined by a BCR-ABL gene fusion, identified in 1960 by Dr. Peter Nowell (Ayatollahi et al., 2018) (Deininger et al., 2000). Before the 1990s, the survival rate for CML within 5 years was less than 30% (Chen et al., 2012). After the Federal Drug Administration (FDA) approved imatinib for CML treatment in 2001, it has over an 80% survival rate 5-10 years after diagnosis (Hochhaus et al., 2017). This demonstrates the great impact of targeted drug design on minimizing CML mortality and that similar approaches using targeted medicine should be undertaken for other malignancies.

Imatinib's Targeted and Non-Targeted Inhibitions

Imatinib was created in the 1990s using rational drug design, a process of creating new medications based on a known biological target, typically with computers (Huggins et al., 2012). It was a landmark medication since it differentiated between cancer and wildtype cells rather than indiscriminately target cells like chemotherapy or radiation treatment (Capdeville et al., 2002). Imatinib is a type II inhibitor specifically designed to target the inactive ABL kinase at the ATP binding site (Gumireddy et al., 2005). It is derived from a 2-phenyl amino pyrimidine with additional pharmacophores added for highly specific interactions with ABL kinase. These groups include a pyridyl group for cell activity, a methyl group for BCR-ABL selectivity, an amide that generally inhibits tyrosine kinases, a benzene to prevent mutagenesis, and an N-methylpiperazine for aqueous solubility and oral bioavailability (Rossari et al., 2018). While imatinib is intended to target the BCR-ABL kinase, because of conserved structures between different ATP binding sites, it interacts with other off-target proteins. However, imatinib demonstrates differential

affinities for various kinases regardless of their sequence similarity (Aleksandrov and Simonson, 2010) (Lin and Roux, 2013). The result is that its use has been expanded to treat other malignancies by inhibiting different proteins in other biological pathways.

Kinases of Interest

Kinases are proteins that facilitate the transfer of a gamma phosphate from nucleotide triphosphates to tyrosine, serine, or threonine of protein substrates (Paul et al., 2020). They are implicated in many biochemical pathways, but their overexpression corresponds with uncontrolled cell growth and division (Bhullar et al., 2018) (Cicenas et al., 2018). The differential charge due to the negatively-charged phosphate induces conformational changes in the proteins, which impacts their ability to conduct biochemical reactions since kinases must adopt specific conformations for pathways to occur (Cohen, 2002) (Sissi and Palumbo, 2009). About 13,000 proteins have phosphorylatable sites (Vlastaridis et al., 2017). This means targeting kinases, which facilitate phosphate transfers, are an interesting target for cancer inhibition. It is possible to get molecular insights into signal transductions based on structural biology and computational simulations of mechanisms (Shah and Kuriyan, 2018).

A 2019 proteomics study from the Wang lab at UC Riverside demonstrates that imatinib affects several kinases' phosphorylation activity (Miao et al., 2019). This potentially reveals new drug targets to explore using computational chemistry techniques. The particular kinases of interest for this project include ABL1, ASK1, AURKA, BRAF, CHK1, FLT3, GSK3β, KIT, LCK, p38α, and SRC; which show substantial changes in phosphorylation activity as a result of imatinib interacting. Of these structures, ABL1, KIT, LCK, p38α, and SRC have available reference structures in the Protein Data Bank for comparison. They will be the focus of this manuscript.

ABL regulates cell differentiation, proliferation, survival, and stress response

ABL1 affects multiple biological pathways including STAT, MYC, RAS, and PI3K; all of which are involved in cell proliferation, epithelial cell formation, and cell survival (Repsold et al., 2017). It is involved in cell differentiation, cell adhesion, and stress responses for DNA repair (Takizawa et al., 2004) (Salles et al., 2011) (Siddiqui et al., 2021). A fusion between the BCR and ABL genes defines CML (Ayatollahi et al., 2018). The effects of ABL inhibition when overexpressed would be a reduction of cell proliferation and uncontrolled cell survival.

KIT mediates cell survival, gamete creation, and cancer development

KIT is a cytokine receptor which precedes several pathways including Ras, Raf, MEK, and ERK in the MAPK signaling cascade and PTEN, Akt, mTOR, and BAD in the PI3K signaling cascade. They are all involved in cell survival, proliferation, and differentiation (Carlino et al., 2014) (Edling and Hallberg, 2007) (Sheikh et al., 2022). It is important in signaling for melanocyte survival, hematopoiesis, the creation of gametes, and regulating many processes involved in cancer development (Brooks, 2006). Overexpression and mutant variants are implicated in cancers (Edling and Hallberg, 2007) (Sheikh et al., 2022). A reduction in KIT overexpression would reduce uncontrolled cell proliferation and growth, and promote better regulation of cancer cell development.

LCK controls immune cell development, survival, and proliferation

LCK regulates T-cell activity and cancer proliferation, survival, and migration via regulation of several pathways including FLT3, IL-7R, BCR, CD28, TCR, CAR, Integrin, NMDA-R, CD55, and PDGF-R and phosphorylates proteins including IL-2-inducible T-cell kinase (ITK), protein kinase C, Phosphoinositide 3-kinase (PI3K), and Zeta-chain-associated protein kinase 70

(ZAP-70) (Bommhardt et al., 2019) (Vahedi et al., 2015) (Elkamhawy et al., 2021) (Rohrs et al., 2016) (Wei et al., 2020). Overexpression of LCK is reported in several tumor types including acute and chronic leukemias and carcinomas of the brain, breast, colon, and prostate (Vahedi et al., 2015) (Elkamhawy et al., 2021) (Singh et al., 2018). Cancer formation increases from low LCK levels due to proliferation of immature immune cells (Elkamhawy et al., 2021) (Singh et al., 2018). Reducing LCK overexpression would correspond with a reduction in various solid cancers, but an excess reduction may result in generation of tumors due to a low production of immune cells.

p38α modulates cell survival, apoptosis, and inflammation responses

Mitogen-activated protein kinases (MAPKs) generally react to stress stimuli such as UV radiation, cytokines, and osmotic shock (Yang et al., 2014) (Asih et al, 2020). p38α (MAPK14) targets substrate proteins like Ahnak, Iws1, Grp78, Pgrmc, Prdx6, and Ranbp2 (Yang et al., 2014). This gives them a substantial role in cell survival, controlled death, proliferation, migration, mRNA stability, and inflammatory responses through cytokine synthesis and inflammatory mediators including TNFα, IL-1β, and COX-2 (Bradham and Mcclay, 2006) (Schieven, 2009) (Young, 2013) (Yang et al., 2014). They control cell maturation, differentiation, apoptosis, and lysosomal degradation pathways (Asih et al, 2020) (Zarubin and Han, 2005) (Bradham and Mcclay, 2006). A reduction in the inappropriate p38α overexpression would enable better responses to stress stimuli, better apoptosis regulation, and removal of dysfunctional cell components.

SRC affects cell adhesion, mobility, differentiation, and apoptosis

SRC regulates multiple pathways including RAS/RAF/MEK/ERK pathways, PI3K/AKT/mTOR pathway, and the STAT3 pathway (Jiao et al., 2018). This gives it a substantial involvement in cell adhesion, mobility, proliferation, and differentiation (Jiao et al., 2018) (Bjorge and Fujita, 2000) (Byeon et al., 2012) (Roskoski, 2004). Increased SRC expression and specific activity corresponds with different cancers including colon and breast cancers. It does so by regulating signals for biological processes like mitogenesis, cytoskeletal organization, growth factor production, apoptosis, inflammation pathways and immunogenic responses (Bjorge and Fujita, 2000) (Byeon et al., 2012) (Ortiz et al., 2021). SRC overexpression promotes several human cancers, particularly when co-overexpressed with epidermal growth factor receptors (Roskoski, 2004) (Ortiz et al., 2021). A better control of SRC expression would correspond with a stronger control over cancerous cell spread, generation, and promotion, especially via controlled cell death (Byeon et al., 2012).

METHODS

Protein Selection

Of the eleven kinases of interest for the project, there are five which have available protein-imatinib bound structures in the Protein Data Bank. These included ABL (PDB ID: 2HYY), KIT (1T46), LCK (2PL0), p38α (3HEC) and SRC kinases (2OIQ). The complexes are multimers, so only the Chain A of the protein, imatinib, and crystal waters were selected for analysis. The crystal waters were retained as they have significant roles mediating hydrogen bonding and protein-drug affinities (Raschke, 2006) (Onuchic and Levy, 2004) (Bellissent-Funel et al., 2016) Only the completed structures for ABL, KIT, and LCK have simulations prepared for analysis as of the writing of this Capstone.

Resolving Protein Structures

Several complexes had missing sections because of high flexibility in loop regions. For smaller gaps of 1-2 residues, an automated SWISS-MODEL technique was used to resolve the missing structures using the primary amino acid sequence (Biasini et al., 2014) (Waterhouse et al., 2018). Larger missing structures were filled in with a copy-paste alignment technique where similar DFG-out protein-drug complexes from structural repositories are superimposed to obtain a conformational sample of the missing loop sequence (Barozet et al., 2021).

Imatinib and Protein Protonation State

The chain A imatinib was isolated for modification. Imatinib is either neutral or protonated at physiological pH as its pKa is 7.7 according to acid-base profiling from titration and nuclear magnetic resonance trials (Szakács et al., 2005). However, imatinib preferentially binds to ABL

in a single protonated (+1) charge state at the piperazinyl group site (Aleksandrov and Simonson, 2009). It is expected that imatinib is protonated when binding with other tyrosine kinases as shown in crystal structures and previous MD literature (Vologzhanina et al., 2020) (Lin et al., 2013). The imatinib was, therefore, protonated using VegaZZ software at the piperazinyl site for all simulations. The chain A proteins were prepared since the protein binding site contains histidines. Previous literature shows that the histidine in ABL was protonated at the epsilon position based on the local environment (Lin and Roux, 2013) (Paul et al., 2020). Other protein histidine protonation sites were not mentioned. Therefore, it is assumed that the AMBER default protonation setting at the epsilon site was used.

Preparing and Running Simulations

The MD simulations were run using AMBER16 for the ABL and LCK and AMBER18 for the KIT. There are no differences between how the two softwares conduct the MD simulations. For each system, FF14SB was used for the protein, GAFF2 was used for the ligand, and TIP3P was used for the water (Maier et al., 2015) (He et al., 2020) (Jorgensen et al., 1983). All simulations are verified models for running MD.

For all drug-protein systems, the simulation box must be neutralized before running the simulations for accurately computing long-range electrostatic calculations (Collier et al., 2019). A minimization is conducted to reduce steric clashes; first hydrogens, then protein side chains, then the whole protein (Kini and Evans, 1991). The ABL-imatinib system was set up using eight sodium ions and one chloride ion to neutralize the net charge of -7 with water box side lengths of 18.45 Å. The LCK-imatinib system was set up using 7 sodium ions and one chloride ion to neutralize the net charge of -6 with water box side lengths of 17.85 Å. The KIT-imatinib system was set up using one sodium ion and five chloride ions to neutralize the net charge of -4 with

water box side lengths of 15.75 Å. To render all drug-protein systems comparable for enthalpy calculations, the ParmEd package was used to remove excess waters from the systems, leaving 22,307 waters in each. The simulations were run for 500 nanoseconds (ns) for the ABL-imatinib and LCK-imatinib kinase systems and 100 ns for KIT-imatinib kinase system.

Analysis Tools

The trajectory files were studied using BIO3D; an R-package for visualizing the root-mean-square-deviation and -fluctuation (RMSD and RMSF) for general protein stability and observing flexible regions, respectively (Grant et al., 2020). Hydrogen bonding data was collected using the Hydrogen Bonds plug-in in Visual Molecular Dynamics (VMD). Protein homology data was extracted using the reference sequences from the NCBI and compared using BLAST.

RESULTS

ABL MD Results

The MD results for ABL show that it stabilizes by 250 ns, with an average RMSD of 2.058 Å and a standard deviation of 0.216 Å. ABL has an average RMSF of 1.099 Å and a standard deviation of 0.756 Å. The hydrogen bonding frequency shows a substantial pattern among residues including GLU52, THR81, MET84, ILE126, HIE127, and ASP147; corresponding with GLU286, THR315, MET318, ILE360, HIS361, and ASP381.

KIT MD Results

The MD results for KIT show that it stabilizes by 55 ns, with an average RMSD of 1.928 Å and a standard deviation of 0.294 Å. KIT has an average RMSF of 0.917 A and a standard deviation of 1.059 Å. The hydrogen bonding frequency shows a substantial pattern among residues including GLU76, THR106, CYS109, ILE153, HIE154, and ASP174; corresponding with GLU640, THR670, CYS673, ILE789, HIE790, and ASP810.

LCK MD Results

The MD results for LCK show that it stabilizes by 75 ns, with an average RMSD of 2.490 A and a standard deviation of 0.299 Å. LCK has an average RMSF of 1.131 A and a standard deviation of 0.778 Å. The hydrogen bonding frequency shows a substantial pattern among residues including GLU58, THR86, and HIE132; corresponding with GLU288, THR316, and HIS362.

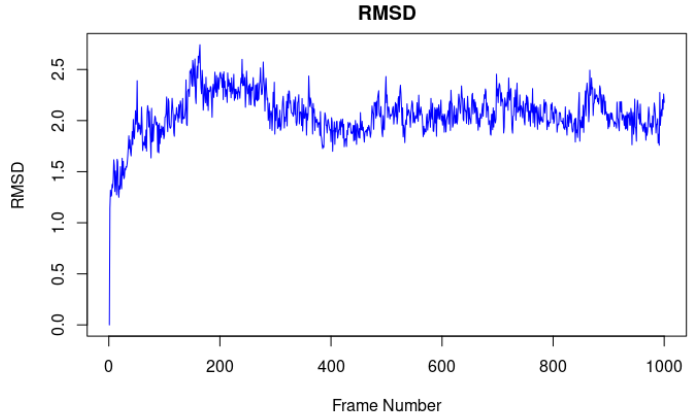

Figure 1. RMSD of ABL over 1000 frames (500 ns)

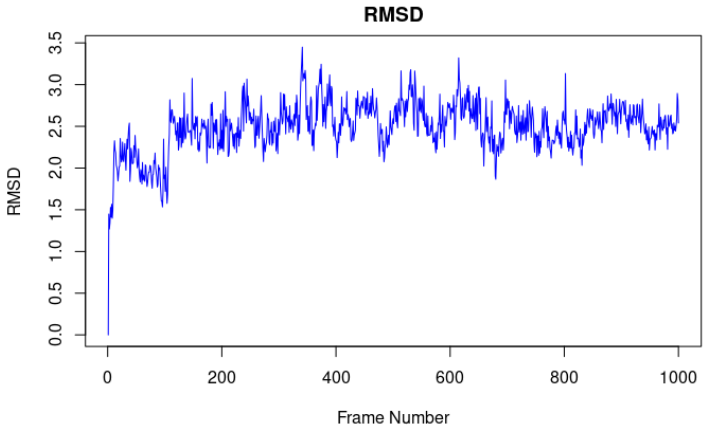

Figure 2. RMSD of LCK over 1000 frames (500 ns)

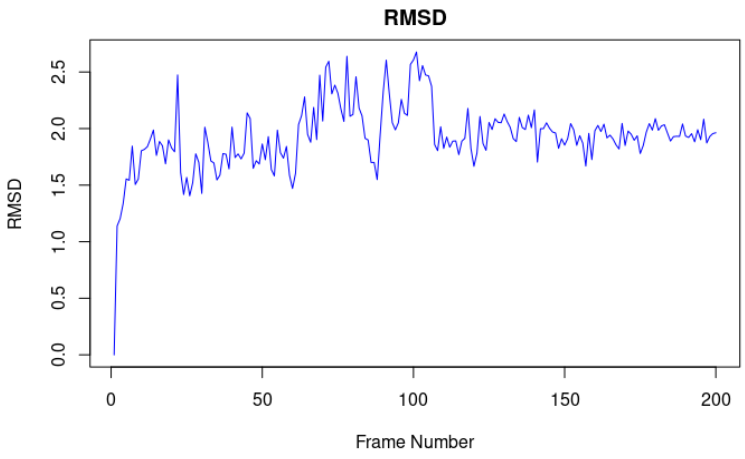

Figure 3. RMSD of KIT over 200 frames (100 ns)

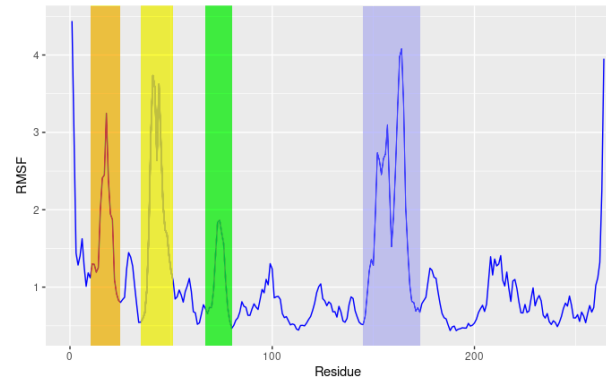

Figure 4. ABL RMSF

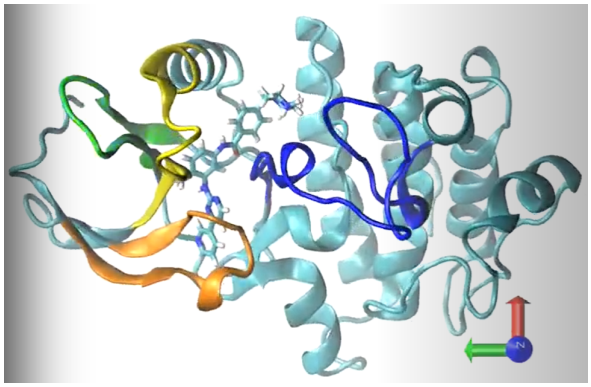

Figure 5. ABL Protein Structure

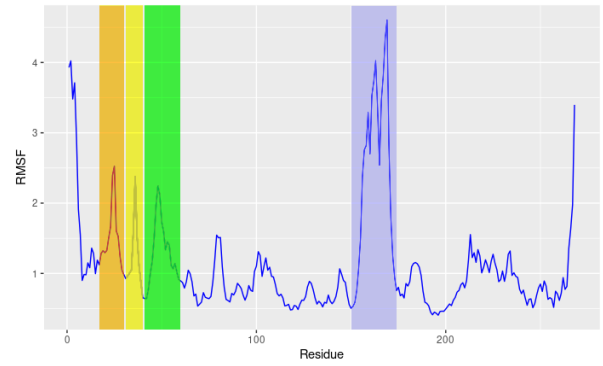

Figure 6. LCK RMSF

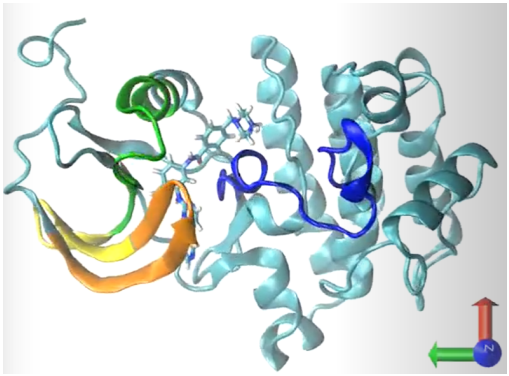

Figure 7. LCK Protein Structure

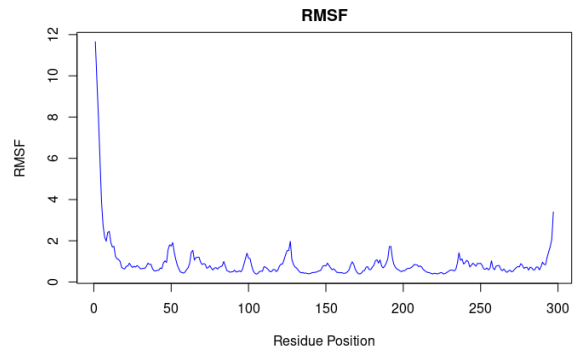

Figure 8. KIT RMSF

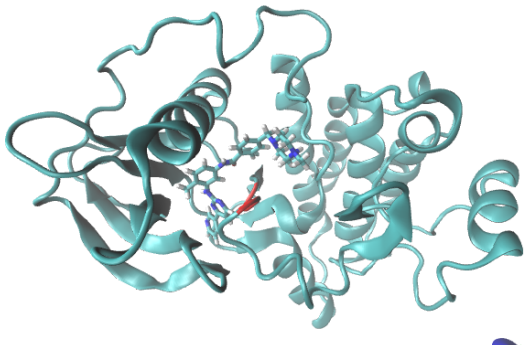

Figure 9. KIT Protein Structure

Table 1. IC_{50} Ranges For ABL, KIT, LCK, p38, and SRC Complexes with Imatinib

Protein-imatinib Complex	IC_{50} ranges (μM)
ABL	0.025 - 0.6
KIT	0.1 - 0.4
LCK	0.32 - 9.0
p38	13.7 - >100
SRC	> 100

Table 2. Hydrogen Bonding Frequency Data of Imatinib-bound ABL, KIT, and LCK Complexes

ABL (ref.)	GLU286	THR315	MET318	ILE360	HIS361	ASP381
	52.80%	49.70%	77.60%	16.00%	31.30%	42.40%
KIT	GLU286	THR315	CYS318	ILE360	HIS361	ASP381
	64.00%	23.50%	73.00%	0.00%	40.50%	6.00%
LCK	GLU286	THR315	MET318	ILE360	HIS361	ASP381
	53.40%	4.50%	0.00%	0.70%	81.70%	0.50%

Table 3. Whole Human Kinase Sequence Identity Comparison

	ABL	KIT	LCK	p38	SRC
ABL		30.7%	44.6%	27.9%	43.9%
KIT			42.7%	34.3%	41.4%
LCK				29.6%	59.9%
p38					28.5%
SRC					

DISCUSSION

Kinase Homology and Drug Affinity

An evaluation of human protein sequence identity from the NCBI data bank using BLASTx shows that all of the proteins have substantial differences in their whole protein sequences. But the residues within 5 Å of imatinib are shown to have high homology with each other, only differing in a few select residues (Aleksandrov and Simonson, 2010). This is expected since imatinib binds into the ATP binding site. The ATP binding site should exhibit high similarity between different proteins because all kinases serve the same general function of transferring gamma phosphates from nucleotide triphosphates to other protein substrates for cell communication and signaling regulation. The high conservation in the binding site, but drastically different IC50 ranges for the imatinib and kinases, shows that there are other structural factors beyond the ATP binding site affecting imatinib's protein affinity.

Kinase Stabilization and Flexibility

A protein's stabilization and flexibility are important because for kinases to function in signaling pathways, they must adopt specific conformations to transfer gamma phosphates from nucleotide triphosphates to the natural substrates on other proteins. Differential flexibilities will affect the kinase's ability to adopt the appropriate confirmation necessary for the signal transduction.

The MD results for ABL show that it forms a stable complex with imatinib. This is indicated early in the simulations at 250 ns with a low average and standard deviation of 2.058 ± 0.216 Å for the RMSD. Previous MD data shows a similar trend with ABL stabilizing early in the simulations at 2 ns with an RMSD of 1 Å (Lin and Roux, 2013). This is not a long enough time-span for analysis of long-scale protein dynamics, but it is consistent with the idea that the

ABL-imatinib complex is highly stable. The MD results show an RMSF of 1.009 ± 0.756 Å. Previous studies show similar RMSF patterns, with high flexibility in the regulatory regions (Lovera et al., 2015).

The MD results for KIT show that it forms a stable complex with imatinib. It is shown in the stabilization of the RMSD at 75 ns, with an average and standard deviation of 1.928 ± 0.294 A. Previous MD data shows a similar trend, with stabilization occurring at 25 ns with an RMSD of 1.45 Å (Gomes et al., 2016). The MD results show an RMSF of 0.917 ± 1.059 Å. The high standard deviation is due to the terminal regions exhibiting high flexibility, but the RMSF of the main kinase domains are all low. These trends are consistent with previous literature, showing low flexibility, and affirming the notion of a stable imatinib-KIT complex (Gomes et al., 2016).

The MD results for LCK show the formation of a stable imatinib-bound complex. The RMSD stabilizes at 100 ns. It has an average and standard deviation of 2.490 ± 0.299 Å. Previous MD studies show an overall stability for LCK at 1.5 Å by 1.75 ns (Lin and Roux, 2013). This is not a long enough time-span for longer timescale protein dynamics, but it is consistent with the observed trends of imatinib-LCK complex stability. The MD results show an RMSF of 1.131 ± 0.778 Å with similar flexibility peaks in key regulatory regions as ABL. There is substantial flexibility at the protein termini contributing to the higher standard deviation. Previous studies show similar peaks for the imatinib-LCK complex as imatinib-ABL, validating the models (Lovera et al., 2015).

Flexible Regions and Contributing Residues of Interest

There are regions which exhibit high flexibility in the proteins including the Walker A motif (P-loop), the DFG motif, the activation loop (A-loop), and the α-C-helix. The P-loop is a motif involved with terminal phosphate transfer and binding (Romero et al., 2018). The DFG motif

marks the start of the activation loop; both of which are involved in the regulation of protein catalysis through the coordination of magnesium ions in the ATP binding site and providing access for substrate binding (Peng et al., 2013) (Dubey and Ojha, 2011) (Modi and Dunbrack, 2019). The α-C-helix is a regulatory element that stabilizes active kinase configurations and aids with efficient catalysis (Taylor and Kornev, 2010).

The MD results for ABL show high RMSF peaks for the P-loop, A-loop, and α-C-helix as shown in figures 4 and 5. This is consistent with previous literature and the known qualities of those regulatory motifs (Lovera et al., 2015). The DFG motif shows little fluctuation, which is expected since the imatinib helps stabilize the DFG-out conformation in the kinases. It may be expected that there will be greater flexibility in the DFG motif in a free-form protein simulation because imatinib will not be present to stabilize the structure. A closer examination of individual residue sequences shows a similarity in the previous data is a local RMSF minima at THR81, which serves as a gatekeeper residue to modulate ligand affinity and avoid protein aggregation (Emrick et al., 2006) (Gibbons et al., 2011). Another notable residue difference is TYR159, which acts as a pseudosubstrate to impair access to the substrate pocket, and exhibits a minimum in the RMSF (Schindler et al., 2000). The minima does not appear in previous literature, which may warrant further investigation from longer simulations.

The MD results for LCK show high RMSF peaks for the P-loop, A-loop, and α-C-helix comparable to the ABL. This is consistent with previous studies demonstrating flexibility for those regulatory motifs (Lovera et al., 2015). The DFG motif shows little fluctuation, which is consistent with the idea that imatinib forms a complex with LCK and stabilizes the DFG-out conformation. A comparison of DFG motif flexibility in a free-form protein simulation may show greater movement because imatinib will not be in the ATP binding pocket. Individual

residues of interest include THR86, which is the gatekeeper residue analogous to THR81 from ABL, which shows a local minimum in the RMSF. Mutants at the gatekeeper position are implicated in imatinib resistance (Lee et al., 2010). Additional data for further individual residues of interest from imatinib-LCK simulations are lacking, representing a future research avenue for longer simulations.

The MD results for KIT exhibit low RMSF peaks for the P-loop, A-loop, and α-C-helix compared to either the ABL or LCK. This is consistent with previous literature, which shows that the flexibility for protein regions in an imatinib-bound KIT complex is generally low (Gomes et al., 2016). Previous data suggests that when imatinib is not bound to the KIT in a free-form protein, that it will exhibit greater flexibility, but not in the regulatory regions. The flexible region corresponds with a flexible loop, of which its biochemical significance warrants further study (Gomes et al., 2016). Because the regions are inflexible, it is difficult to ascertain particular residues of interest at this time.

Imatinib Hydrogen Bonding Patterns Show Homology in ATP Pocket

Most kinase residues in the ATP binding pocket are homologous in the different systems, including those which form hydrogen bonds with imatinib in a bound complex. An analysis of hydrogen bonding frequency data from MD shows that ABL forms six key hydrogen bonds with imatinib at residues GLU286, THR315, MET318, ILE360, HIS361, and ASP381 with frequencies of 52.8%, 49.7%, 77.6%, 16.0%, 31.3%, and 42.4%; respectively. These interaction frequencies are consistent with previous data showing that imatinib forms hydrogen bonds at those residues (Avendaño and Menéndez, 2015) (Lin and Roux, 2013). A comparison of the homologous residues for KIT and LCK were investigated. The MD data for KIT shows that it forms hydrogen bonds with GLU286, THR315, MET318, HIS361, and ASP381 with frequencies

of 64.0%, 23.5%, 73.0%, 40.5%, and 6.0%; respectively. These hydrogen bonds are expected as observed in previous literature (Mol et al., 2004) (Lin and Roux, 2013) (Keretsu et al., 2020). The MD results for LCK show that it forms hydrogen bonds for GLU286, THR315, and HIS361 with frequencies of 53.4%, 4.5%, and 81.7%; respectively. These hydrogen bonds are observed in previous literature; further validating the experimental results (Lin and Roux, 2013).

IC_{50} Values Correlate with Known Affinity Ranges

The IC_{50} value describes the concentration of ligand required to inhibit a protein's biological functions by 50%. The smaller the value, the lower the concentration of ligand required to inhibit the protein, and vice versa. ABL exhibits an IC_{50} range of approximately 0.025 - 0.6 μM as validated by multiple previous studies (Zin et al., 2020) (Seeliger et al., 2007) (Deininger et al., 2005) (Lovera et al., 2015) (Dar et al., 2009) (Kitagawa et al., 2013) (Namboodiri et al., 2010). This makes sense since imatinib was designed to find into ABL's ATP binding site. KIT has an IC_{50} range of approximately 0.1 μM to 0.4 μM, exhibiting a similar binding and inhibition capacity for imatinib as ABL (Seeliger et al., 2007) (Lovera et al., 2015) (Paniagua et al., 2006) (Kitagawa et al., 2013) (Namboodiri et al., 2010) (Ravichandran et al., 2015). This is consistent with previous observations showing that imatinib can favorably bind with KIT, enabling its use to treat gastrointestinal stromal tumors by inhibiting KIT. LCK shows an IC_{50} range of approximately 0.32 μM to 9.0 μM, which is a substantially higher range compared to either ABL or KIT (Seggewiss et al., 2005) (Lee et al., 2010) (Lin and Roux, 2013) (Druker et al., 2005) (Lovera et al., 2015) (Buchdunger et al., 2001) (Kitagawa et al., 2013) (Namboodiri et al., 2010) (Ravichandran et al., 2015). This is consistent with kinetics observations showing that LCK has a lower affinity for imatinib than either ABL or KIT. p38α has an IC50 range between 13.7 μM to over 100 μM according to previous literature (Namboodiri et al., 2010) (Chen et al., 2008)

(Dietrich et al., 2010). This is consistent with previous kinetics studies showing that p38α has a generally low affinity for imatinib. SRC has been repeatedly validated to have an IC_{50} value exceeding 100 micromolar according to previous literature, showing it has poor affinity with imatinib (Druker et al., 2005) (Lovera et al., 2015) (Seeliger et al., 2007) (Dar et al., 2009) (Namboodiri et al., 2010) (Ravichandran et al., 2015). This is consistent with previous studies showing that SRC has a 2400x worse affinity for imatinib compared to ABL. Explaining the differences in binding affinity is of substantial importance for rational drug design, as understanding why some medicines bind to proteins better than others will help guide the creation of new drugs that specifically bind one or a few proteins to prevent unwanted side effects and expand treatment options for other malignancies.

Expectations for Future Simulations

If other kinases have similar homology with the ABL binding site, one may expect similar hydrogen bonding patterns. However, as shown with previous literature and MD results, this is not always the case. Even over the 500 ns simulations for ABL and LCK, homologous hydrogen bonds did not form with comparable frequency. It is, therefore, necessary to conduct further MD simulations on known systems to evaluate the accuracy identifying non-covalent interactions before expanding the simulation to kinases without imatinib-bound complexes in the PDB.

Previous literature shows that p38α forms an unstable complex with imatinib (Yang et al., 2011). Available RMSD data over 10 ns shows a continual increase in the protein and pocket, indicating a lack of overall stability (Yang et al., 2011). The RMSF shows similar flexibilities for ABL and LCK in the kinase regulatory regions (Yang et al., 2011). Imatinib has been shown to form non-covalent interactions with MET109, THR106, GLU71, and ASP168 (Namboodiri et al., 2010). This is consistent with the observation of imatinib having a high IC_{50} value range from

13.7 μM to over 100 μM; a substantially higher range than ABL, KIT, or LCK. If there is a weak affinity between imatinib and p38, a statistically similar RMSD and RMSF should be observed between the free-form and imatinib-bound complexes because of weak non-covalent hydrogen bonding effects. If there are substantial differences, it would indicate that imatinib's presence in the binding pocket is affecting p38α's dynamics, but that there are other structural factors explaining its weak affinity for p38α.

Previous literature shows that imatinib has a 2400x weaker binding affinity for SRC compared to ABL. The RMSD from previous studies shows imatinib-SRC complex formation, stabilizing at around 1.2 Å by 2.5 ns (Lin and Roux, 2013). The RMSF differences between the free-form and imatinib-bound complexes are comparable within ± 0.5 Å, with the most difference in the regulatory motif of the P-loop (Morando et al., 2016). SRC is expected to form four hydrogen bonds with GLU310, THR338, MET341, and ASP404 (Seeliger et al., 2009). This is consistent with the known IC_{50} range in previous studies, with all known observations ranking over 100 μM. If there is a weak affinity between imatinib and SRC, a statistically similar RMSD and RMSF should be observed between the free-form and imatinib-bound complexes because of weak non-covalent hydrogen bonding effects. If there are substantial differences, it would indicate that imatinib's presence in the binding pocket is affecting SRC's dynamics, but that there are other structural factors explaining its weak affinity for SRC.

Future Directions

Comparing Free-form and Imatinib-bound Kinase Dynamics

Analyzing the dynamics differences between the free-form and imatinib-bound complex states will show how the imatinib binding affects the stability and flexibility differences for the protein.

It would generally be expected that those proteins which form a strong complex with imatinib will exhibit substantial differences in the stability and flexibility findings. Those proteins which do not form strong complexes with imatinib will show insignificant differences in the stability and flexibility (Karch et al., 2019). The estimation of the differences in Gibbs binding free energy requires long MD simulations to compare the unbound and bound equilibrium states (Salo-Ahen et al., 2020) (Hata et al., 2021). The simulations will be expanded to p38α and SRC kinases, along with free-form simulations of ABL, KIT, LCK, p38α, and SRC for experimental verification. The simulations will then be expanded to other kinases of interest including ASK1, AURKA, BRAF, CHK1, FLT3, and GSK3 beta; all of which exhibit changes in kinase phosphorylation with imatinib present (Miao et al., 2019). Of these kinases without available imatinib-bound complexes in the PDB, only AURKA has available MD data showing it forms a stable complex based on RMSD, showing it may be a promising target for further study (Zhang et al., 2019). However, detailed insights into protein dynamics are lacking, representing future research opportunities.

Investigating Bridge Waters and Salt Bridges

Crystal waters have a critical role in stabilizing biomolecular complexes and aiding protein folding (Petukhov et al., 1999) (Onuchic and Levy, 2004) (Bellissent-Funel et al., 2016) (Steinke et al., 2018). Water molecules in imatinib-bound ABL MD simulations have been previously explored, but the simulations were conducted for only 14 ns, which is not long enough to track key bridge waters over a longer time scale (Dubey and Ojha, 2011). The findings, however, suggest that hydration plays an important role in mediating the imatinib-protein complex. Previous MD data consistently shows the importance of salt bridges, another type of non-covalent interaction, in mediating kinase promiscuity and intra-protein interactions between

different regulatory motifs (Dubey and Ojha, 2011) (Keretsu et al., 2020) (Hanson et al., 2019). Studies suggest that while salt bridges do not significantly affect kinase activity, they generally increase complex entropy, which should be reflected in thermodynamics analysis and free energy calculations (Dubey and Ojha, 2011). It is, therefore, of importance to investigate how hydration effects and salt bridge interactions help mediate the free energy in the imatinib-bound complexes.

Evaluating Imatinib Docking Energies

Molecular docking is a useful method to evaluate the possible conformations that a ligand may adopt when bound to a protein (Pantsar and Poso, 2018). It is especially powerful when combined with structural biology to explain what non-covalent interactions or binding pocket conformations contribute to binding affinity differences between ligands and proteins (Forli et al., 2016). However, there are limitations in how the software selects conformations and if similar structures are missing. Docking works by calculating and ranking the energetic favorability of the ligand-protein complex rather than by a binding mechanism (Pantsar and Poso, 2018) (Forli et al., 2016). It is possible to obtain drug conformations that are energetically favorable, but not biologically possible in a protein. It is, therefore, useful to consider a few of the top selections instead of only the most favorable and to compare the structures with similar complexes, such as the same drug bound to different proteins or similar drugs bound to the same protein (Ramirez and Caballero, 2018). Docking tools cannot accurately estimate binding energies, but they are still useful for a general evaluation of binding affinity trends, even if they do not perfectly agree with experimental kinetics (Pantsar and Poso, 2018). AutoDock software will be used to dock imatinib with different protein conformations collected from MD to check how structural changes over time affect the binding energies. Imatinib will be cross-docked to

DFG-out kinase structures without available imatinib-bound complexes and the most reasonable conformation from visual examination will be used for MD (Ravichandran et al., 2015) (Chen et al., 2019) (Ramirez and Caballero, 2018).

Principal Component and Dihedral Correlation Analysis

As MD yields large coordinate data for each atom in the run, it is useful to use principal component analysis (PCA) to determine the essential protein dynamics and construct a free energy landscape (Padhi et al., 2022) (David and Jacobs, 2013) (Sittel et al., 2014). PCA is a method to simplify correlated observations to principal components (PCs), identifying important conformational changes that either repeat or do not repeat over time (David and Jacobs, 2013). PCA standardizes the variable range to the same scale to not bias the results, computes a covariance or correlation matrix to check for direct and inverse correlations, determines the PCs with linear algebra to discern the variables with greatest variance, and plots them such that each PC represents a line that maximizes variance while being uncorrelated with subsequent PCs (Lever et al., 2017) (Jolliffe and Cadima, 2016). For MD, the structure must be aligned to a reference to minimize translation and rotation motion (David and Jacobs, 2013). The degrees of freedom, corresponding with the PCs, depends on the protein size and atom selection, but it will be three times the number of atoms selected corresponding to the x-, y- and z-axes (David and Jacobs, 2013) (Srikumar et al., 2014). The BIO3D R package can calculate and visualize PCA, making it a useful tool for future research (Grant et al., 2020). Since PCA is reducing variables in the set, there is a slight accuracy reduction, but identification of important protein motions is easier without irrelevant data.

Dihedral angles form between four atoms connected linearly and they define the protein's conformational dynamics over an MD simulation (Long and Tian, 2016). Protein dynamics are

important for their functions physiologically, but are difficult to track, so a solution is dihedral correlation analysis (Taddese et al., 2020). Dihedral correlations are useful for separating internal and whole protein motion when interpreting free energy landscapes, describing the total molecular energy of a system, and coordination between individual residues and larger secondary structures (Taddese et al., 2020) (Altis et al., 2007) (Friederich et al., 2018) (Moulick and Chakrabarti, 2022) (Haddad et al., 2019). They have an advantage over conventional PCA since dihedrals are affected by Van der Waal interactions, hydrogen bonding with other residues and waters, and salt bridge interactions; presenting another avenue for guiding rational drug design (Taddese et al., 2020). A tool for studying dihedral distributions is T-Analyst, an in-house Linux program developed by the Chang lab to study the dihedrals of protein backbones, side-chains, and ligands (Ai et al., 2010). Dihedral correlation analysis is useful in conjunction with PCA to solve for the important free-form and imatinib-bound protein dynamics and energetics as the simulation progresses producing large coordinate and dihedral data sets.

Dissociation Simulations, Residence Time, and Binding Affinity Approximation

After analyzing the free-form and imatinib-bound MD simulations, a future goal of the project is to study dissociation simulations. This is to measure the residence time, the inverse of the dissociation rate constant k_{off} and the time required for a drug to unbind from a protein, which is a better predictor of drug efficacy (Sohraby and Nunves-Alves, 2023). As drug dissociation from a protein takes place over a longer time period than is obtainable from a single simulation, it is necessary to use alternate techniques to lengthen the simulations while conserving computational power (Re et al., 2019). Milestoning theory is a technique to enhance computational simulations of kinetics using shorter MD trajectories to approximate the solution using free energy calculations and mean first passage time (Elber et al., 2020) (Elber, 2020). Previous studies have

shown that imatinib exits ABL via two mechanisms, either sliding under the alpha-C-helix or exiting under the P-loop via a hinge mechanism, which are the same pathways by which it is known to associate with ABL (Yang et al., 2009) (Paul et al., 2020) (Narayan et al., 2021) (Shekhar et al., 2022). KIT kinase has imatinib dissociate via the ATP channel, though the precise unbinding mechanism is unexplored (Yang et al., 2009). All other kinases in this study do not have available literature exploring the imatinib unbinding mechanism, though if they have lower affinities compared to ABL and KIT, a general trend of faster dissociation should be reflected in the simulations (Shah and Kuriyan, 2018). It is of interest to explore the structural factors that impede imatinib's retention in the ATP binding pocket to guide rational drug design.

REFERENCES

Ai, R.; Qaiser Fatmi, M.; Chang, C. A. T-Analyst: A Program for Efficient Analysis of Protein Conformational Changes by Torsion Angles. *J. Comput.-Aided Mol. Des.* **2010**, *24* (10), 819–827. DOI:10.1007/s10822-010-9376-y.

Aleksandrov, A.; Simonson, T. A Molecular Mechanics Model for Imatinib and Imatinib:Kinase Binding. *J. Comput. Chem.* **2009**, *31* (7), 1550–1560. DOI:10.1002/jcc.21442.

Aleksandrov, A.; Simonson, T. Molecular Dynamics Simulations Show That Conformational Selection Governs the Binding Preferences of Imatinib for Several Tyrosine Kinases. *J. Biol. Chem.* **2010**, *285* (18), 13807–13815. DOI:10.1074/jbc.m110.109660.

Altis, A.; Nguyen, P. H.; Hegger, R.; Stock, G. Dihedral Angle Principal Component Analysis of Molecular Dynamics Simulations. *J. Chem. Phys.* **2007**, *126* (24), 244111. DOI:10.1063/1.2746330.

Ashburn, T. T.; Thor, K. B. Drug Repositioning: Identifying and Developing New Uses for Existing Drugs. *Nat. Rev. Drug Discovery* **2004**, *3* (8), 673–683. DOI:10.1038/nrd1468.

Asih, P. R.; Prikas, E.; Stefanoska, K.; Tan, A. R.; Ahel, H. I.; Ittner, A. Functions of P38 MAP Kinases in the Central Nervous System. *Front. Mol. Neurosci.* **2020**, *13*, 1–27. DOI:10.3389/fnmol.2020.570586.

Avendaño, C.; Menéndez, J. C. Drugs That Inhibit Signaling Pathways for Tumor Cell Growth and Proliferation. *Medicinal Chemistry of Anticancer Drugs* **2015**, 391–491. DOI:10.1016/b978-0-444-62649-3.00010-7.

Ayatollahi, H.; Keramati, M. R.; Shirdel, A.; Kooshyar, M. M.; Raiszadeh, M.; Shakeri, S.; Sadeghian, M. H. BCR-ABL Fusion Genes and Laboratory Findings in Patients with Chronic Myeloid Leukemia in Northeast Iran. *Caspian J. Intern. Med.* **2018**, *9* (1), 65–70. DOI:10.22088/cjim.9.1.65.

Barozet, A.; Chacón, P.; Cortés, J. Current Approaches to Flexible Loop Modeling. *Curr. Res. Struct. Biol.* **2021**, *3*, 187–191. DOI:10.1016/j.crstbi.2021.07.002.

Bellissent-Funel, M.-C.; Hassanali, A.; Havenith, M.; Henchman, R.; Pohl, P.; Sterpone, F.; van der Spoel, D.; Xu, Y.; Garcia, A. E. Water Determines the Structure and Dynamics of Proteins. *Chem. Rev.* **2016**, *116* (13), 7673–7697. DOI:10.1021/acs.chemrev.5b00664.

Bhullar, K. S.; Lagarón, N. O.; McGowan, E. M.; Parmar, I.; Jha, A.; Hubbard, B. P.; Rupasinghe, H. P. Kinase-Targeted Cancer Therapies: Progress, Challenges and Future Directions. *Mol. Cancer* **2018**, *17* (1). DOI:10.1186/s12943-018-0804-2.

Biasini, M.; Bienert, S.; Waterhouse, A.; Arnold, K.; Studer, G.; Schmidt, T.; Kiefer, F.; Cassarino, T. G.; Bertoni, M.; Bordoli, L.; Schwede, T. Swiss-Model: Modelling Protein Tertiary and Quaternary Structure Using Evolutionary Information. *Nucleic Acids Res.* **2014**, *42* (W1), 252–258. DOI:10.1093/nar/gku340.

Bjorge, J. D.; Jakymiw, A.; Fujita, D. J. Selected Glimpses into the Activation and Function of Src Kinase. *Oncogene* **2000**, *19* (49), 5620–5635. DOI:10.1038/sj.onc.1203923.

Bommhardt, U.; Schraven, B.; Simeoni, L. Beyond TCR Signaling: Emerging Functions of Lck in Cancer and Immunotherapy. *Int. J. Mol. Sci.* **2019**, *20* (14), 1–18. DOI:10.3390/ijms20143500.

Bradham, C.; McClay, D. R. P38 MAPK in Development and Cancer. *Cell Cycle* **2006**, *5* (8), 824–828. DOI:10.4161/cc.5.8.2685.

Brooks, S. A. Studies of Genetic Variation at the Kit Locus and White Spotting Patterns in the Horse. https://uknowledge.uky.edu/gradschool_diss/479 (accessed 2023-05-11).

Buchdunger, E.; Matter, A.; Druker, B. J. BCR-ABL Inhibition as a Modality of CML Therapeutics. *Biochim. Biophys. Acta, Rev. Cancer* **2001**, *1551* (1), 11–18. DOI:10.1016/s0304-419x(01)00022-1.

Byeon, S. E.; Yi, Y.-S.; Oh, J.; Yoo, B. C.; Hong, S.; Cho, J. Y. The Role of Src Kinase in Macrophage-Mediated Inflammatory Responses. *Mediators Inflammation* **2012**, *2012*, 1–18. DOI:10.1155/2012/512926.

Capdeville, R.; Buchdunger, E.; Zimmermann, J.; Matter, A. Glivec (STI571, Imatinib), a Rationally Developed, Targeted Anticancer Drug. *Nat. Rev. Drug Discovery* **2002**, *1* (7), 493–502. DOI:10.1038/nrd839.

Carlino, M. S.; Todd, J. R.; Rizos, H. Resistance to C-KIT Inhibitors in Melanoma: Insights for Future Therapies. *Oncoscience* **2014**, *1* (6), 423–426. DOI:10.18632/oncoscience.51.

Chen, N.; Bürli, R. W.; Neira, S.; Hungate, R.; Zhang, D.; Yu, V.; Nguyen, Y.; Tudor, Y.; Plant, M.; Flynn, S.; Meagher, K. L.; Lee, M. R.; Zhang, X.; Itano, A.; Schrag, M.; Xu, Y.; Ng, G. Y.; Hu, E. Discovery of a Potent and Selective C-KIT Inhibitor for the Treatment of Inflammatory Diseases. *Bioorg. Med. Chem. Lett.* **2008**, *18* (14), 4137–4141. DOI:10.1016/j.bmcl.2008.05.089.

Chen, X.; Liu, H.; Xie, W.; Yang, Y.; Wang, Y.; Fan, Y.; Hua, Y.; Zhu, L.; Zhao, J.; Lu, T.; Chen, Y.; Zhang, Y. Investigation of Crystal Structures in Structure-Based Virtual Screening for Protein Kinase Inhibitors. *J. Chem. Inf. Model.* **2019**, *59* (12), 5244–5262. DOI:10.1021/acs.jcim.9b00684.

Chen, Y.; Wang, H.; Kantarjian, H.; Cortes, J. Trends in Chronic Myeloid Leukemia Incidence and Survival in the United States from 1975 to 2009. *Leuk. Lymphoma* **2012**, *54* (7), 1411–1417. DOI:10.3109/10428194.2012.745525.

Cicenas, J.; Zalyte, E.; Bairoch, A.; Gaudet, P. Kinases and Cancer. *Cancers* **2018**, *10* (3), 1-7. DOI:10.3390/cancers10030063.

Cohen, P. The Origins of Protein Phosphorylation. *Nat. Cell Biol.* **2002**, *4* (5), 127–130. DOI:10.1038/ncb0502-e127.

Collier, T. A.; Piggot, T. J.; Allison, J. R. Molecular Dynamics Simulation of Proteins. *Methods Mol. Biol.* **2019**, *2073*, 311–327. DOI:10.1007/978-1-4939-9869-2_17.

Dar, A. C.; Lopez, M. S.; Shokat, K. M. Small Molecule Recognition of C-Src via the Imatinib-Binding Conformation. *Chem. Biol.* **2008**, *15* (10), 1015–1022. DOI:10.1016/j.chembiol.2008.09.007.

David, C. C.; Jacobs, D. J. Principal Component Analysis: A Method for Determining the Essential Dynamics of Proteins. *Protein Dynamics* **2013**, 193–226. DOI:10.1007/978-1-62703-658-0_11.

Deininger, M. W.; Goldman, J. M.; Melo, J. V. The Molecular Biology of Chronic Myeloid Leukemia. *Blood* **2000**, *96* (10), 3343–3356. DOI:10.1182/blood.v96.10.3343.

Deininger, M.; Buchdunger, E.; Druker, B. J. The Development of Imatinib as a Therapeutic Agent for Chronic Myeloid Leukemia. *Blood* **2005**, *105* (7), 2640–2653. DOI:10.1182/blood-2004-08-3097.

Dietrich, J.; Hulme, C.; Hurley, L. H. The Design, Synthesis, and Evaluation of 8 Hybrid DFG-out Allosteric Kinase Inhibitors: A Structural Analysis of the Binding Interactions of Gleevec®, Nexavar®, and BIRB-796. *Bioorg. Med. Chem.* **2010**, *18* (15), 5738–5748. DOI:10.1016/j.bmc.2010.05.063.

Druker, B. J. Imatinib as a Paradigm of Targeted Therapies. *Adv. Cancer Res.* **2004**, *91*, 1–30. DOI:10.1016/s0065-230x(04)91001-9.

Dubey, K. D.; Ojha, R. P. Conformational Flexibility, Binding Energy, Role of Salt Bridge and Alanine-Mutagenesis for C-Abl Kinase Complex. *J. Mol. Model.* **2011**, *18* (5), 1679–1689. DOI:10.1007/s00894-011-1199-9.

Edling, C. E.; Hallberg, B. C-Kit—a Hematopoietic Cell Essential Receptor Tyrosine Kinase. *Int. J. Biochem. Cell Biol.* **2007**, *39* (11), 1995–1998. DOI:10.1016/j.biocel.2006.12.005.

Elber, R. Milestoning: An Efficient Approach for Atomically Detailed Simulations of Kinetics in Biophysics. *Annu. Rev. Biophys.* **2020**, *49* (1), 69–85. DOI:10.1146/annurev-biophys-121219-081528.

Elber, R.; Fathizadeh, A.; Ma, P.; Wang, H. Modeling Molecular Kinetics with Milestoning. *Wiley Interdiscip. Rev.: Comput. Mol. Sci.* **2020**, *11* (4). DOI:10.1002/wcms.1512.

Elkamhawy, A.; Ali, E. M.; Lee, K. New Horizons in Drug Discovery of Lymphocyte-Specific Protein Tyrosine Kinase (LCK) Inhibitors: A Decade Review (2011–2021) Focussing on Structure–Activity Relationship (SAR) and Docking Insights. *J. Enzyme Inhib. Med. Chem.* **2021**, *36* (1), 1572–1600. DOI:10.1080/14756366.2021.1937143.

Emrick, M. A.; Lee, T.; Starkey, P. J.; Mumby, M. C.; Resing, K. A.; Ahn, N. G. The Gatekeeper Residue Controls Autoactivation of ERK2 via a Pathway of Intramolecular Connectivity. *Proc. Natl. Acad. Sci.* **2006**, *103* (48), 18101–18106. DOI:10.1073/pnas.0608849103.

Forli, S.; Huey, R.; Pique, M. E.; Sanner, M. F.; Goodsell, D. S.; Olson, A. J. Computational Protein–Ligand Docking and Virtual Drug Screening with the Autodock Suite. *Nat. Protoc.* **2016**, *11* (5), 905–919. DOI:10.1038/nprot.2016.051.

Friederich, P.; Konrad, M.; Strunk, T.; Wenzel, W. Machine Learning of Correlated Dihedral Potentials for Atomistic Molecular Force Fields. *Sci. Rep.* **2018**, *8* (1). DOI:10.1038/s41598-018-21070-0.

Gibbons, D. L.; Pricl, S.; Kantarjian, H.; Cortes, J.; Quintás-Cardama, A. The Rise and Fall of Gatekeeper Mutations? The BCR-ABL1 T315I Paradigm. *Cancer* **2011**, *118* (2), 293–299. DOI:10.1002/cncr.26225.

Gomes, P. D. S. F. C.; Chauvot De Beauchêne, I.; Panel, N.; Lopez, S.; De Sepulveda, P.; Geraldo Pascutti, P.; Solary, E.; Tchertanov, L. Insight on Mutation-Induced Resistance

from Molecular Dynamics Simulations of the Native and Mutated CSF-1R and Kit. *PLOS ONE* **2016**, *11* (7), 1–25. DOI:10.1371/journal.pone.0160165.

Granatowicz, A.; Piatek, C. I.; Moschiano, E.; El-Hemaidi, I.; Armitage, J. D.; Akhtari, M. An Overview and Update of Chronic Myeloid Leukemia for Primary Care Physicians. *Korean J. Fam. Med.* **2015**, *36* (5), 197. DOI:10.4082/kjfm.2015.36.5.197.

Grant, B. J.; Skjærven, L.; Yao, X. The Bio3D Packages for Structural Bioinformatics. *Protein Sci.* **2020**, *30* (1), 20–30. DOI:10.1002/pro.3923.

Gumireddy, K.; Baker, S. J.; Cosenza, S. C.; John, P.; Kang, A. D.; Robell, K. A.; Reddy, M. V.; Reddy, E. P. A Non-ATP-Competitive Inhibitor of BCR-ABL Overrides Imatinib Resistance. *Proc. Natl. Acad. Sci.* **2005**, *102* (6), 1992–1997. DOI:10.1073/pnas.0408283102.

Haddad, Y.; Adam, V.; Heger, Z. Rotamer Dynamics: Analysis of Rotamers in Molecular Dynamics Simulations of Proteins. *Biophys. J.* **2019**, *116* (11), 2062–2072. DOI:10.1016/j.bpj.2019.04.017.

Hanson, S. M.; Georghiou, G.; Thakur, M. K.; Miller, W. T.; Rest, J. S.; Chodera, J. D.; Seeliger, M. A. What Makes a Kinase Promiscuous for Inhibitors? *Cell Chem. Biol.* **2019**, *26* (3), 390–399. DOI:10.1016/j.chembiol.2018.11.005.

Hata, H.; Phuoc Tran, D.; Marzouk Sobeh, M.; Kitao, A. Binding Free Energy of Protein/Ligand Complexes Calculated Using Dissociation Parallel Cascade Selection Molecular Dynamics and Markov State Model. *Biophys. Physicobiol.* **2021**, *18* (0), 305–316. DOI:10.2142/biophysico.bppb-v18.037.

He, X.; Man, V. H.; Yang, W.; Lee, T.-S.; Wang, J. A Fast and High-Quality Charge Model for the next Generation General Amber Force Field. *J. Chem. Phys.* **2020**, *153* (11), 1–11. DOI:10.1063/5.0019056.

Hochhaus, A.; Larson, R. A.; Guilhot, F.; Radich, J. P.; Branford, S.; Hughes, T. P.; Baccarani, M.; Deininger, M. W.; Cervantes, F.; Fujihara, S.; Ortmann, C.-E.; Menssen, H. D.; Kantarjian, H.; O'Brien, S. G.; Druker, B. J. Long-Term Outcomes of Imatinib Treatment for Chronic Myeloid Leukemia. *N. Engl. J. Med.* **2017**, *376* (10), 917–927. DOI:10.1056/nejmoa1609324.

Huggins, D. J.; Sherman, W.; Tidor, B. Rational Approaches to Improving Selectivity in Drug Design. *J. Med. Chem.* **2012**, *55* (4), 1424–1444. DOI:10.1021/jm2010332.

Jabbour, E.; Kantarjian, H. Chronic Myeloid Leukemia: 2020 Update on Diagnosis, Therapy and Monitoring. *Am. J. Hematol.* **2020**, *95* (6), 691–709. DOI:10.1002/ajh.25792.

Jiao, Q.; Bi, L.; Ren, Y.; Song, S.; Wang, Q.; Wang, Y. Advances in Studies of Tyrosine Kinase Inhibitors and Their Acquired Resistance. *Mol. Cancer* **2018**, *17* (1), 1–12. DOI:10.1186/s12943-018-0801-5.

Jolliffe, I. T.; Cadima, J. Principal Component Analysis: A Review and Recent Developments. *Philos. Trans. R. Soc., A.* **2016**, *374* (2065), 20150202. DOI:10.1098/rsta.2015.0202.

Jorgensen, W. L. The Many Roles of Computation in Drug Discovery. *Science* **2004**, *303* (5665), 1813–1818. DOI:10.1126/science.1096361.

Jorgensen, W. L.; Chandrasekhar, J.; Madura, J. D.; Impey, R. W.; Klein, M. L. Comparison of Simple Potential Functions for Simulating Liquid Water. *J. Chem. Phys.* **1983**, *79* (2), 926–935. DOI:10.1063/1.445869.

Karch, R.; Stocsits, C.; Ilieva, N.; Schreiner, W. Intramolecular Domain Movements of Free and Bound PMHC and TCR Proteins: A Molecular Dynamics Simulation Study. *Cells* **2019**, *8* (7), 720. DOI:10.3390/cells8070720.

Keretsu, S.; Ghosh, S.; Cho, S. J. Molecular Modeling Study of C-KIT/PDGFRA Dual Inhibitors for the Treatment of Gastrointestinal Stromal Tumors. *Int. J. Mol. Sci.* **2020**, *21* (21), 1–25. DOI:10.3390/ijms21218232.

Kini, R. M.; Evans, H. J. Molecular Modeling of Proteins: A Strategy for Energy Minimization by Molecular Mechanics in the Amber Force Field. *J. Biomol. Struct. Dyn.* **1991**, *9* (3), 475–488. DOI:10.1080/07391102.1991.10507930.

Kinnings, S. L.; Liu, N.; Buchmeier, N.; Tonge, P. J.; Xie, L.; Bourne, P. E. Drug Discovery Using Chemical Systems Biology: Repositioning the Safe Medicine Comtan to Treat Multi-Drug and Extensively Drug Resistant Tuberculosis. *PLoS Comput. Biol.* **2009**, *5* (7), 1–10. DOI:10.1371/journal.pcbi.1000423.

Kitagawa, D.; Yokota, K.; Gouda, M.; Narumi, Y.; Ohmoto, H.; Nishiwaki, E.; Akita, K.; Kirii, Y. Activity-Based Kinase Profiling of Approved Tyrosine Kinase Inhibitors. *Genes Cells* **2012**, *18* (2), 110–122. DOI:10.1111/gtc.12022.

Lawrence, S. Drug Output Slows in 2006. *Nat. Biotechnol.* **2007**, *25* (10), 1073–1073. DOI:10.1038/nbt1007-1073.

Lee, K. C.; Ouwehand, I.; Giannini, A. L.; Thomas, N. S.; Dibb, N. J.; Bijlmakers, M. J. Lck Is a Key Target of Imatinib and Dasatinib in T-Cell Activation. *Leukemia* **2010**, *24* (4), 896–900. DOI:10.1038/leu.2010.11.

Lever, J.; Krzywinski, M.; Altman, N. Principal Component Analysis. *Nat. Methods* **2017**, *14* (7), 641–642. DOI:10.1038/nmeth.4346.

Levy, Y.; Onuchic, J. N. Water and Proteins: A Love–Hate Relationship. *Proc. Natl. Acad. Sci.* **2004**, *101* (10), 3325–3326. DOI:10.1073/pnas.0400157101.

Lin, Y.-L.; Meng, Y.; Jiang, W.; Roux, B. Explaining Why Gleevec Is a Specific and Potent Inhibitor of ABL Kinase. *Proc. Natl. Acad. Sci.* **2013**, *110* (5), 1664–1669. DOI:10.1073/pnas.1214330110.

Lin, Y.-L.; Roux, B. Computational Analysis of the Binding Specificity of Gleevec to ABL, c-Kit, Lck, and c-Src Tyrosine Kinases. *J. Am. Chem. Soc.* **2013**, *135* (39), 14741–14753. DOI:10.1021/ja405939x.

Long, S.; Tian, P. Shot Range and High Order Correlations in Proteins. https://arxiv.org/abs/1607.03764 (accessed 2023-05-11).

Lovera, S.; Morando, M.; Pucheta-Martinez, E.; Martinez-Torrecuadrada, J. L.; Saladino, G.; Gervasio, F. L. Towards a Molecular Understanding of the Link between Imatinib Resistance and Kinase Conformational Dynamics. *PLoS Comput. Biol.* **2015**, *11* (11), 1–19. DOI:10.1371/journal.pcbi.1004578.

Maier, J. A.; Martinez, C.; Kasavajhala, K.; Wickstrom, L.; Hauser, K. E.; Simmerling, C. FF14SB: Improving the Accuracy of Protein Side Chain and Backbone Parameters from Ff99sb. *J. Chem. Theory Comput.* **2015**, *11* (8), 3696–3713. DOI:10.1021/acs.jctc.5b00255.

Miao, W.; Guo, L.; Wang, Y. Imatinib-Induced Changes in Protein Expression and ATP-Binding Affinities of Kinases in Chronic Myelocytic Leukemia Cells. *Anal. Chem.* **2019**, *91* (5), 3209–3214. DOI:10.1021/acs.analchem.9b00289.

Modi, V.; Dunbrack, R. L. Defining a New Nomenclature for the Structures of Active and Inactive Kinases. *Proc. Natl. Acad. Sci.* **2019**, *116* (14), 6818–6827. DOI:10.1073/pnas.1814279116.

Mol, C. D.; Dougan, D. R.; Schneider, T. R.; Skene, R. J.; Kraus, M. L.; Scheibe, D. N.; Snell, G. P.; Zou, H.; Sang, B.-C.; Wilson, K. P. Structural Basis for the Autoinhibition and STI-571 Inhibition of c-Kit Tyrosine Kinase. *J. Biol. Chem.* **2004**, *279* (30), 31655–31663. DOI:10.1074/jbc.m403319200.

Morando, M. A.; Saladino, G.; D'Amelio, N.; Pucheta-Martinez, E.; Lovera, S.; Lelli, M.; López-Méndez, B.; Marenchino, M.; Campos-Olivas, R.; Gervasio, F. L. Conformational Selection and Induced Fit Mechanisms in the Binding of an Anticancer Drug to the C-Src Kinase. *Sci. Rep.* **2016**, *6* (1), 1–9. DOI:10.1038/srep24439.

Moulick, A. G.; Chakrabarti, J. Correlated Dipolar and Dihedral Fluctuations in a Protein. *Chem. Phys. Lett.* **2022**, *797*, 139574. DOI:10.1016/j.cplett.2022.139574.

Namboodiri, H. V.; Bukhtiyarova, M.; Ramcharan, J.; Karpusas, M.; Lee, Y.; Springman, E. B. Analysis of Imatinib and Sorafenib Binding to P38α Compared with C-ABL and B-RAF Provides Structural Insights for Understanding the Selectivity of Inhibitors Targeting the DFG-out Form of Protein Kinases. *Biochemistry* **2010**, *49* (17), 3611–3618. DOI:10.1021/bi100070r.

Narayan, B.; Buchete, N.-V.; Elber, R. Computer Simulations of the Dissociation Mechanism of Gleevec from ABL Kinase with Milestoning. *J. Phys. Chem. B* **2021**, *125* (22), 5706–5715. DOI:10.1021/acs.jpcb.1c00264.

Ortiz, M. A.; Mikhailova, T.; Li, X.; Porter, B. A.; Bah, A.; Kotula, L. Src Family Kinases, Adaptor Proteins and the Actin Cytoskeleton in Epithelial-to-Mesenchymal Transition. *Cell Commun. Signaling* **2021**, *19* (1), 1–19. DOI:10.1186/s12964-021-00750-x.

Padhi, A. K.; Janežič, M.; Zhang, K. Y. J. Molecular Dynamics Simulations: Principles, Methods, and Applications in Protein Conformational Dynamics. *Advances in Protein Molecular and Structural Biology Methods* **2022**, 439–454. DOI:10.1016/b978-0-323-90264-9.00026-x.

Paniagua, R. T.; Sharpe, O.; Ho, P. P.; Chan, S. M.; Chang, A.; Higgins, J. P.; Tomooka, B. H.; Thomas, F. M.; Song, J. J.; Goodman, S. B.; Lee, D. M.; Genovese, M. C.; Utz, P. J.; Steinman, L.; Robinson, W. H. Selective Tyrosine Kinase Inhibition by Imatinib Mesylate for the Treatment of Autoimmune Arthritis. *J. Clin. Invest.* **2006**, *116* (10), 2633–2642. DOI:10.1172/jci28546.

Pantsar, T.; Poso, A. Binding Affinity via Docking: Fact and Fiction. *Molecules* **2018**, *23* (8), 1899. DOI:10.3390/molecules23081899.

Paul, F.; Thomas, T.; Roux, B. Diversity of Long-Lived Intermediates along the Binding Pathway of Imatinib to ABL Kinase Revealed by MD Simulations. *J. Chem. Theory Comput.* **2020**, *16* (12), 7852–7865. DOI:10.1021/acs.jctc.0c00739.

Paul, S. M.; Mytelka, D. S.; Dunwiddie, C. T.; Persinger, C. C.; Munos, B. H.; Lindborg, S. R.; Schacht, A. L. How to Improve R&D Productivity: The Pharmaceutical Industry's Grand Challenge. *Nat. Rev. Drug Discovery* **2010**, *9* (3), 203–214. DOI:10.1038/nrd3078.

Peng, Y.-H.; Shiao, H.-Y.; Tu, C.-H.; Liu, P.-M.; Hsu, J. T.-A.; Amancha, P. K.; Wu, J.-S.; Coumar, M. S.; Chen, C.-H.; Wang, S.-Y.; Lin, W.-H.; Sun, H.-Y.; Chao, Y.-S.; Lyu, P.-C.; Hsieh, H.-P.; Wu, S.-Y. Protein Kinase Inhibitor Design by Targeting the ASP-Phe-Gly (DFG) Motif: The Role of the DFG Motif in the Design of Epidermal Growth Factor Receptor Inhibitors. *J. Med. Chem.* **2013**, *56* (10), 3889–3903. DOI:10.1021/jm400072p.

Petukhov, M.; Cregut, D.; Soares, C. M.; Serrano, L. Local Water Bridges and Protein Conformational Stability. *Protein Sci.* **1999**, *8* (10), 1982–1989. DOI:10.1110/ps.8.10.1982.

Rahman, M. Antimicrobial Secondary Metabolites—Extraction, Isolation, Identification, and Bioassay. *Evidence-Based Validation of Herbal Medicine* **2015**, 495–513. DOI:10.1016/b978-0-12-800874-4.00023-4.

Ramírez, D.; Caballero, J. Is It Reliable to Take the Molecular Docking Top Scoring Position as the Best Solution without Considering Available Structural Data? *Molecules* **2018**, *23* (5), 1038. DOI:10.3390/molecules23051038.

Raschke, T. M. Water Structure and Interactions with Protein Surfaces. *Curr. Opin. Struct. Biol.* **2006**, *16* (2), 152–159. DOI:10.1016/j.sbi.2006.03.002.

Ravichandran, S.; Luke, B. T.; Collins, J. R. Can Structural Features of Kinase Receptors Provide Clues on Selectivity and Inhibition? A Molecular Modeling Study. *J. Mol. Graphics Modell.* **2015**, *57*, 36–48. DOI:10.1016/j.jmgm.2014.12.007.

Re, S.; Oshima, H.; Kasahara, K.; Kamiya, M.; Sugita, Y. Encounter Complexes and Hidden Poses of Kinase-Inhibitor Binding on the Free-Energy Landscape. *Proc. Natl. Acad. Sci.* **2019**, *116* (37), 18404–18409. DOI:10.1073/pnas.1904707116.

Repsold, L.; Pool, R.; Karodia, M.; Tintinger, G.; Joubert, A. M. An Overview of the Role of Platelets in Angiogenesis, Apoptosis and Autophagy in Chronic Myeloid Leukaemia. *Cancer Cell Int.* **2017**, *17* (1), 1–12. DOI:10.1186/s12935-017-0460-4.

Rohrs, J. A.; Wang, P.; Finley, S. D. Predictive Model of Lymphocyte-Specific Protein Tyrosine Kinase (LCK) Autoregulation. *Cell. Mol. Bioeng.* **2016**, *9* (3), 351–367. DOI:10.1007/s12195-016-0438-7.

Romero, M. L. R.; Yang, F.; Lin, Y.-R.; Toth-Petroczy, A.; Berezovsky, I. N.; Goncearenco, A.; Yang, W.; Wellner, A.; Kumar-Deshmukh, F.; Sharon, M.; Baker, D.; Varani, G.; Tawfik, D. S. Simple yet Functional Phosphate-Loop Proteins. *Proc. Natl. Acad. Sci.* **2018**, *115* (51), 11943–11950. DOI:10.1073/pnas.1812400115.

Roskoski, R. SRC Protein–Tyrosine Kinase Structure and Regulation. *Biochem. Biophys. Res. Commun.* **2004**, *324* (4), 1155–1164. DOI:10.1016/j.bbrc.2004.09.171.

Rossari, F.; Minutolo, F.; Orciuolo, E. Past, Present, and Future of BCR-ABL Inhibitors: From Chemical Development to Clinical Efficacy. *J. Hematol. Oncol.* **2018**, *11* (1). DOI:10.1186/s13045-018-0624-2.

Salo-Ahen, O. M.; Alanko, I.; Bhadane, R.; Bonvin, A. M.; Honorato, R. V.; Hossain, S.; Juffer, A. H.; Kabedev, A.; Lahtela-Kakkonen, M.; Larsen, A. S.; Lescrinier, E.; Marimuthu, P.; Mirza, M. U.; Mustafa, G.; Nunes-Alves, A.; Pantsar, T.; Saadabadi, A.; Singaravelu, K.; Vanmeert, M. Molecular Dynamics Simulations in Drug Discovery and Pharmaceutical Development. *Processes* **2020**, *9* (1), 71. DOI:10.3390/pr9010071.

Salles, D.; Mencalha, A. L.; Ireno, I. C.; Wiesmüller, L.; Abdelhay, E. BCR-ABL Stimulates Mutagenic Homologous DNA Double-Strand Break Repair via the DNA-End-Processing Factor CTIP. *Carcinogenesis* **2010**, *32* (1), 27–34. DOI:10.1093/carcin/bgq216.

Schieven, G. The P38α Kinase Plays a Central Role in Inflammation. *Curr. Top. Med. Chem.* **2009**, *9* (11), 1038–1048. DOI:10.2174/156802609789630974.

Schindler, T.; Bornmann, W.; Pellicena, P.; Miller, W. T.; Clarkson, B.; Kuriyan, J. Structural Mechanism for STI-571 Inhibition of Abelson Tyrosine Kinase. *Science* **2000**, *289* (5486), 1938–1942. DOI:10.1126/science.289.5486.1938.

Seeliger, M. A.; Nagar, B.; Frank, F.; Cao, X.; Henderson, M. N.; Kuriyan, J. C-Src Binds to the Cancer Drug Imatinib with an Inactive ABL/c-Kit Conformation and a Distributed

Thermodynamic Penalty. *Structure* **2007**, *15* (3), 299–311. DOI:10.1016/j.str.2007.01.015.

Seeliger, M. A.; Ranjitkar, P.; Kasap, C.; Shan, Y.; Shaw, D. E.; Shah, N. P.; Kuriyan, J.; Maly, D. J. Equally Potent Inhibition of C-Src and ABL by Compounds That Recognize Inactive Kinase Conformations. *Cancer Res.* **2009**, *69* (6), 2384–2392. DOI:10.1158/0008-5472.can-08-3953.

Seggewiss, R.; Wiestner, A.; Dunbar, C. E.; Douek, D. C.; Price, D. A.; Magnusson, M. K.; Greiner, E.; Lore, K. Imatinib Inhibits T-Cell Receptor-Mediated T-Cell Proliferation and Activation in a Dose-Dependent Manner. *Blood* **2005**, *105* (6), 2473–2479. DOI:10.1182/blood-2004-07-2527.

Shah, N. H.; Kuriyan, J. Understanding Molecular Mechanisms in Cell Signaling through Natural and Artificial Sequence Variation. *Nat. Struct. Mol. Biol.* **2018**, *26* (1), 25–34. DOI:10.1038/s41594-018-0175-9.

Sheikh, E.; Tran, T.; Vranic, S.; Levy, A.; Bonfil, R. D. Role and Significance of C-Kit Receptor Tyrosine Kinase in Cancer: A Review. *Bosnian J. Basic Med. Sci.* **2022**, *22* (5), 683–698. DOI:10.17305/bjbms.2021.7399.

Shekhar, M.; Smith, Z.; Seeliger, M. A.; Tiwary, P. Protein Flexibility and Dissociation Pathway Differentiation Can Explain Onset of Resistance Mutations in Kinases**. *Angew. Chem.* **2022**, *134* (28), 1–9. DOI:10.1002/ange.202200983.

Siddiqui, A.; Tumiati, M.; Joko, A.; Sandholm, J.; Roering, P.; Aakko, S.; Vainionpää, R.; Kaipio, K.; Huhtinen, K.; Kauppi, L.; Tuomela, J.; Hietanen, S. Targeting DNA

Homologous Repair Proficiency with Concomitant Topoisomerase II and C-ABL Inhibition. *Front. Oncol.* **2021**, *11*, 1–16. DOI:10.3389/fonc.2021.733700.

Singh, P. K.; Kashyap, A.; Silakari, O. Exploration of the Therapeutic Aspects of LCK: A Kinase Target in Inflammatory Mediated Pathological Conditions. *Biomed. Pharmacother.* **2018**, *108*, 1565–1571. DOI:10.1016/j.biopha.2018.10.002.

Sissi, C.; Palumbo, M. Effects of Magnesium and Related Divalent Metal Ions in Topoisomerase Structure and Function. *Nucleic Acids Res.* **2009**, *37* (3), 702–711. DOI:10.1093/nar/gkp024.

Sittel, F.; Jain, A.; Stock, G. Principal Component Analysis of Molecular Dynamics: On the Use of Cartesian vs. Internal Coordinates. *J. Chem. Phys.* **2014**, *141* (1), 014111. DOI:10.1063/1.4885338.

Sohraby, F.; Nunes-Alves, A. Advances in Computational Methods for Ligand Binding Kinetics. *Trends Biochem. Sci.* **2023**, *48* (5), 437–449. DOI:10.1016/j.tibs.2022.11.003.

Srikumar, P. S.; Rohini, K.; Rajesh, P. K. Molecular Dynamics Simulations and Principal Component Analysis on Human Laforin Mutation W32G and W32G/K87a. *Protein J.* **2014**, *33* (3), 289–295. DOI:10.1007/s10930-014-9561-2.

Steinke, N.; Genina, A.; Gillams, R. J.; Lorenz, C. D.; McLain, S. E. Proline and Water Stabilization of a Universal Two-Step Folding Mechanism for β-Turn Formation in Solution. *J. Am. Chem. Soc.* **2018**, *140* (23), 7301–7312. DOI:10.1021/jacs.8b03643.

Szakács, Z.; Béni, S.; Varga, Z.; Örfi, L.; Kéri, G.; Noszál, B. Acid−base Profiling of Imatinib (Gleevec) and Its Fragments. *J. Med. Chem.* **2004**, *48* (1), 249–255. DOI:10.1021/jm049546c.

Taddese, B.; Garnier, A.; Abdi, H.; Henrion, D.; Chabbert, M. Deciphering Collaborative Sidechain Motions in Proteins during Molecular Dynamics Simulations. *Sci. Rep.* **2020**, *10* (1). DOI:10.1038/s41598-020-72766-1.

Takizawa, Y.; Kinebuchi, T.; Kagawa, W.; Yokoyama, S.; Shibata, T.; Kurumizaka, H. Mutational Analyses of the Human RAD51-Tyr315 Residue, a Site for Phosphorylation in Leukaemia Cells. *Genes Cells* **2004**, *9* (9), 781–790. DOI:10.1111/j.1365-2443.2004.00772.x.

Taylor, S. S.; Kornev, A. P. Protein Kinases: Evolution of Dynamic Regulatory Proteins. *Trends Biochem. Sci.* **2011**, *36* (2), 65–77. DOI:10.1016/j.tibs.2010.09.006.

Vahedi, S.; Chueh, F.-Y.; Chandran, B.; Yu, C.-L. Lymphocyte-Specific Protein Tyrosine Kinase (LCK) Interacts with CR6-Interacting Factor 1 (CRIF1) in Mitochondria to Repress Oxidative Phosphorylation. *BMC Cancer* **2015**, *15* (1), 1–14. DOI:10.1186/s12885-015-1520-6.

Vlastaridis, P.; Kyriakidou, P.; Chaliotis, A.; Van de Peer, Y.; Oliver, S. G.; Amoutzias, G. D. Estimating the Total Number of Phosphoproteins and Phosphorylation Sites in Eukaryotic Proteomes. *GigaScience* **2017**, *6* (2), 1–11. DOI:10.1093/gigascience/giw015.

Vologzhanina, A. V.; Ushakov, I. E.; Korlyukov, A. A. Intermolecular Interactions in Crystal Structures of Imatinib-Containing Compounds. *Int. J. Mol. Sci.* **2020**, *21* (23), 1–16. DOI:10.3390/ijms21238970.

Waterhouse, A.; Bertoni, M.; Bienert, S.; Studer, G.; Tauriello, G.; Gumienny, R.; Heer, F. T.; de Beer, T. A. P.; Rempfer, C.; Bordoli, L.; Lepore, R.; Schwede, T. Swiss-Model: Homology Modelling of Protein Structures and Complexes. *Nucleic Acids Res.* **2018**, *46* (W1). DOI:10.1093/nar/gky427.

Wei, Q.; Brzostek, J.; Sankaran, S.; Casas, J.; Hew, L. S.-Q.; Yap, J.; Zhao, X.; Wojciech, L.; Gascoigne, N. R. Lck Bound to Coreceptor Is Less Active than Free Lck. *Proc. Natl. Acad. Sci.* **2020**, *117* (27), 15809–15817. DOI:10.1073/pnas.1913334117.

Yang, L.-J.; Zou, J.; Xie, H.-Z.; Li, L.-L.; Wei, Y.-Q.; Yang, S.-Y. Steered Molecular Dynamics Simulations Reveal the Likelier Dissociation Pathway of Imatinib from Its Targeting Kinases C-Kit and Abl. *PLoS ONE* **2009**, *4* (12). DOI:10.1371/journal.pone.0008470.

Yang, Y.; Kim, S. C.; Yu, T.; Yi, Y.-S.; Rhee, M. H.; Sung, G.-H.; Yoo, B. C.; Cho, J. Y. Functional Roles of P38 Mitogen-Activated Protein Kinase in Macrophage-Mediated Inflammatory Responses. *Mediators Inflammation* **2014**, *2014*, 1–13. DOI:10.1155/2014/352371.

Yang, Y.; Shen, Y.; Liu, H.; Yao, X. Molecular Dynamics Simulation and Free Energy Calculation Studies of the Binding Mechanism of Allosteric Inhibitors with P38α Map Kinase. *J. Chem. Inf. Model.* **2011**, *51* (12), 3235–3246. DOI:10.1021/ci200159g.

Young, P. R. Perspective on the Discovery and Scientific Impact of P38 Map Kinase. *SLAS Discovery* **2013**, *18* (10), 1156–1163. DOI:10.1177/1087057113497401.

Zarubin, T.; Han, J. Activation and Signaling of the P38 Map Kinase Pathway. *Cell Res.* **2005**, *15* (1), 11–18. DOI:10.1038/sj.cr.7290257.

Zhang, Z.; Xu, Y.; Wu, J.; Shen, Y.; Cheng, H.; Xiang, Y. Exploration of the Selective Binding Mechanism of Protein Kinase Aurora a Selectivity via a Comprehensive Molecular Modeling Study. *PeerJ* **2019**, *7*. DOI:10.7717/peerj.7832.

Zin, P. P. K.; Borrel, A.; Fourches, D. Benchmarking 2D/3D/MD-QSAR Models for Imatinib Derivatives: How Far Can We Predict? *J. Chem. Inf. Model.* **2020**, *60* (7), 3342–3360. DOI:10.1021/acs.jcim.0c00200.